

# A NUMERICAL ANALYSIS OF THE DYNAMICS OF A TENSEGRITY-MEMBRANE STRUCTURE

Teixeira, L.H.\* , Izuka, J.H.\*\* , Gonzalez, P.\* , Kurka, P.\*

Faculty of Mechanical Engineering - UNICAMP\* , Faculty of Applied Sciences - UNICAMP\*\*

**Keywords:** *Finite Element Method, Tensegrity, Structure Dynamics, Lightweight Structures*

## Abstract

*A form-finding method for the tensegrity structure is used in order to find the pretensions and final configuration of the structure. A finite element mesh with the pretension consideration is used to model the structure. A numerical modal analysis is performed over the structure and comparisons is made between tensegrity and tensegrity-membrane structures. A static analysis over a finite element model of a membrane is performed in order to account for pretension in the modal analysis. The membrane model is compared with an experimental data obtained in [1] to validate the model.*

## 1 Introduction

According to Fuller [2], a tensegrity structure can be understood as an assembly of components under traction and compression organized in a discontinuously compressed system. In [3] and [4], tensegrity is defined as a structure that keeps a steady volume in space by means of discontinuous elements under compression (bars) connected to a continuous web of tensioned elements (cables). Kenneth D. Snelson, however, registered in 1965 the patent of a structure made by long members put separately, either under tension or compression, to form a grid. In this structure, the compressed members were put apart from each other while the tensioned members were interconnected to form a continuous tension web [5]. This Snelson's invention came to be called *tensegrity* in the future.

The advantage of these structures is that they can be designed so their elements are stressed in one direction only. This characteristic not only simplifies the motion equations but leads to more precise models. Furthermore, these unidirectional stresses permit a more efficient material selection, leading to mass reductions of the structure [6].

Tensegrity-membrane is an extension of the tensegrity studies. They are formed by membranes, bars and tendons. This kind of structures inherit typical advantages of classical tensegrity systems, such as reduced masses, extreme flexibility and the ability to change its shape [7]. This ability is useful for retractile structures, enabling numerous space applications. In the deployed form, these structures are more resistant to the launching related complications. On the other hand, in the expanded configuration, the structure will bear the orbital loads only, which are sharply lower [8]. Furthermore, this kind of function dismisses the risky assembly of structures in space.

## 2 Methods

A tensegrity structure is composed by nodes and members, that are related by the connectivity matrix, shown in [6], as can be seen by Equation 1. The nodes are the extremities of the elements while the members are the elements itself.

$$\mathbf{n}_i \in \mathbb{R}^3 \quad (1)$$

The matrix  $\mathbf{N}$  contains the node coordinates of the structure. The vector  $\mathbf{x}$ ,  $\mathbf{y}$ , and  $\mathbf{z}$  are the nodes in the x, y, and z axis respectively. These

coordinates are organized as follows:

$$\mathbf{N} = \begin{Bmatrix} \mathbf{n}_1 \\ \vdots \\ \mathbf{n}_n \end{Bmatrix} = [\mathbf{x} \quad \mathbf{y} \quad \mathbf{z}] \quad (2)$$

The members ( $\mathbf{m}_k$ ) are the length of the element in each axis and can be written as:

$$\mathbf{m}_k = \mathbf{n}_{ik} - \mathbf{n}_{jk} \quad (3)$$

where the terms  $\mathbf{n}_{ik}$  and  $\mathbf{n}_{jk}$  are the  $i^{th}$  and  $j^{th}$  nodes of the  $k^{th}$  member.

The matrix  $\mathbf{M}$  contains the members  $\mathbf{m}_k$  as follows:

$$\mathbf{M} = \begin{Bmatrix} \mathbf{m}_1 \\ \vdots \\ \mathbf{m}_m \end{Bmatrix} \quad (4)$$

The matrices  $\mathbf{M}$  and  $\mathbf{N}$  are related by the connectivity matrix  $\mathbf{C}$ :

$$\mathbf{C} \cdot \mathbf{N} = \mathbf{M} \quad (5)$$

and [9]:

$$\mathbf{C} \cdot \mathbf{x} = \mathbf{u} \quad (6)$$

$$\mathbf{C} \cdot \mathbf{y} = \mathbf{v} \quad (7)$$

$$\mathbf{C} \cdot \mathbf{z} = \mathbf{w} \quad (8)$$

where  $\mathbf{u}$ ,  $\mathbf{v}$  and  $\mathbf{w}$  are the length of the members in the x, y and z axis, respectively.

To obtain the equilibrium equation, it must introduce the force density ( $q$ ) concept. The force density is the ratio between the traction or compression forces and the length of the members. That relation is shown in the equation 9 to an arbitrary member  $k$ :

$$q_k = \frac{s_k}{l_k} \quad (9)$$

where  $s_k$  and  $l_k$  is the axial force and length of member  $k$ , respectively.

The equilibrium matrix ( $\mathbf{E}$ ) can be obtained by Equation 10.

$$\mathbf{E} = \mathbf{C}^T \mathbf{Q} \mathbf{C} \quad (10)$$

where,

$$\mathbf{Q} = \text{diag}(\mathbf{q}) \quad (11)$$

It can be written the equilibrium equation in nodes coordinates function. For structures with fixations, the equilibrium equations are:

$$\begin{cases} \mathbf{E} \cdot \mathbf{x} + \mathbf{E}^f \mathbf{x}^f = \mathbf{0} \\ \mathbf{E} \cdot \mathbf{y} + \mathbf{E}^f \mathbf{y}^f = \mathbf{0} \\ \mathbf{E} \cdot \mathbf{z} + \mathbf{E}^f \mathbf{z}^f = \mathbf{0} \end{cases} \quad (12)$$

where  $f$  is the vector with the fixed nodes of the system. For structures without fixations, the equations would be:

$$\begin{cases} \mathbf{E} \cdot \mathbf{x} = \mathbf{0} \\ \mathbf{E} \cdot \mathbf{y} = \mathbf{0} \\ \mathbf{E} \cdot \mathbf{z} = \mathbf{0} \end{cases} \quad (13)$$

Equations 12 and 13 can be solved predetermining the values of the force densities.

### 2.0.1 Form-finding method

In order to work with tensegrity structures, it is necessary to find the structure's equilibrium shape. There's the analytical approach used by [10] and a nonlinear method used by [11]. In this study, it's used the force density method, which will be explained in the next section.

The concept of force density and its advantages is presented in one of Schek's works [12]. However, the method has some disadvantages, as there are few restrictions on the final shape of the structure to be determined, although some methods to restrain the final form exist. This disadvantage is due to the input of the model being only the force density and some predetermined nodes.

### 2.0.2 Condition of non-degeneracy

As shown in [9], in order for the structure to have  $n_d$  dimensions, the matrix  $\mathbf{E}_{n \times n}$  must have the condition presented below:

$$\text{rank}(\mathbf{E}_{n \times n}) = n - h' \quad (14)$$

where,

$$h' = n_d + 1 \quad (15)$$

Choosing the force density values that will result in a matrix  $\mathbf{E}$  that has the required rank is one of the difficulties of finding the final form of the structure. In [13], three types of processes are mentioned. The first would be the intuitive method, which could be used in simple systems with few members. The second process would be the analytical method, in which the analysis of the matrix results in expressions that can relate the force densities.

The third process would be the iterative method, where the force density values are updated at each iteration until the equilibrium matrix ( $\mathbf{E}$ ) reaches the desired rank. This method will be described in the next topic.

### 2.0.3 Iterative method for the form-finding

In [9] and [14], is proposed an iterative method in order to obtain the desired rank of the equilibrium matrix.

First, initial values are selected for the force density ( $q^i$ ) vector, that is used to obtain the equilibrium matrix  $\mathbf{E}$  through Equations 10 and 11. Then, the eigenvectors and eigenvalues of  $\mathbf{E}$  are obtained through Equation 16.

$$\mathbf{E} = \Phi^T \Lambda \Phi \quad (16)$$

In order to the rank of  $\mathbf{E}$  has the value presented in Equation 14, the number of zeros between eigenvalues of  $\Lambda$  must be  $h'$ . In the iterative method it's analyzed the number of zeros in the diagonal of matrix  $\Lambda$ . If the required number is not met, the lower values of the diagonal is replaced by zero to reach the required value.

Proceeding with the iterative method, a new  $\Lambda$  value is found with the substitution of the  $h'$  smaller values with zero. This new  $\Lambda$  will be denoted as  $\bar{\Lambda}$  and it's used to find  $\bar{\mathbf{E}}$  through Equation 16.

With Equation 20, one can obtain the updated value of  $\bar{\mathbf{q}}$  through the matrix  $\bar{\mathbf{E}}$ . one can get  $\bar{\mathbf{q}}$ , which are the updated values of force densities. For this, one must define the matrices  $\mathbf{R}$  and  $\mathbf{g}$ .

$\mathbf{R}_i$  is given by:

$$\mathbf{R}_i \cdot \mathbf{q} = \mathbf{E}_i \quad (17)$$

where  $\mathbf{E}_i$  is the  $i^{th}$  column of  $\mathbf{E}$ .

Then:

$$\mathbf{R}^T = (\mathbf{R}_1^T; \dots; \mathbf{R}_i^T; \dots; \mathbf{R}_n^T) \quad (18)$$

Also,  $\mathbf{g}$  is given by:

$$\mathbf{g}^T = (\mathbf{E}_1^T; \dots; \mathbf{E}_i^T; \dots; \mathbf{E}_n^T) \quad (19)$$

Then,  $\bar{\mathbf{q}}$  can be obtained by the Equation 20.

$$\bar{\mathbf{q}} = (\mathbf{R}^T \mathbf{R})^{-1} \mathbf{R}^T \mathbf{g} \quad (20)$$

The updated force density matrix ( $\mathbf{E}^{i+1}$ ) is obtained with  $\bar{\mathbf{q}}$  and the Equation 10. Then,  $\Lambda^{i+1}$ , which is the updated value of matrix  $\Lambda$ , is obtained with Equation 16. The iterative procedure is repeated until the required number of zeros in  $\Lambda^{i+1}$  is achieved.

It is still possible to add some restriction conditions of the force density relations in the final form of the structure. This restriction can be written as presented below:

$$\mathbf{F} \mathbf{q} = \mathbf{0} \quad (21)$$

where the matrix  $\mathbf{F}$  relates the force density components of the vector  $\mathbf{q}$ .

The node's height of the tensegrity structure can be determined by the Equation 22 as seen in [14].

$$\mathbf{C}^T \text{diag}(\mathbf{C} \mathbf{z}) \mathbf{q} = \mathbf{0} \quad (22)$$

The restrictions presented above can be written as the following linear equation system:

$$\begin{pmatrix} \mathbf{F} \\ \mathbf{C}^T \text{diag}(\mathbf{C} \mathbf{z}) \end{pmatrix} \mathbf{q} = \mathbf{G} \mathbf{q} = \mathbf{0} \quad (23)$$

The system's solution is given by:

$$\mathbf{q} = \phi(\mathbf{R} \phi)^{-1} \mathbf{g} \quad (24)$$

where  $\phi$  is the null space of  $\mathbf{G}$ .

These constraints can be accounted in the iterative method by using the Equation 24 instead of Equation 20 in order to find  $\bar{\mathbf{q}}$ .

With the force density vector determined, it's necessary to find the final form of the structure. Thus, to find the nodal coordinates  $\mathbf{X}$ , the homogeneous Equation 25 is solved.

$$\mathbf{H}\mathbf{X} = \mathbf{0} \quad (25)$$

where,

$$\mathbf{H} = \begin{bmatrix} \mathbf{E} & \mathbf{O}_n & \mathbf{O}_n \\ \mathbf{O}_n & \mathbf{E} & \mathbf{O}_n \\ \mathbf{E} & \mathbf{O}_n & \mathbf{E} \end{bmatrix} \quad (26)$$

$$\mathbf{X} = \begin{Bmatrix} \mathbf{x} \\ \mathbf{y} \\ \mathbf{z} \end{Bmatrix} \quad (27)$$

The solution for the Equation 25, as shown in [9], is given by:

$$\mathbf{X} = \mathbf{A}\mathbf{A}^{-1}\bar{\mathbf{X}} \quad (28)$$

where  $\mathbf{A}$  is the null space of  $\mathbf{H}$  and  $\bar{\mathbf{A}}$  is the corresponding components in  $\mathbf{A}$  of related to the independent set of nodal coordinates  $\bar{\mathbf{X}}$ .

The Figure 1 shows the form-finding procedure that was used.

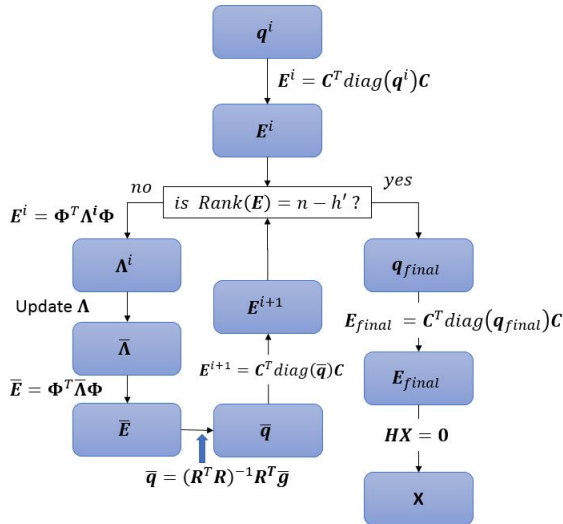


**Fig. 1** Iterative process to find force density vector values.

#### 2.0.4 Form-finding of the Tensegrity-Membrane structure

The traction in each tendon is found by the form-finding method described in this paper. The finite element method can be used in order to find the membrane displacements and stress that can represent the same effect of the tendons of the structure without membrane that was found. Thus, the tendons can be replaced by the membranes with no changes in the positions of the nodes of the structure.

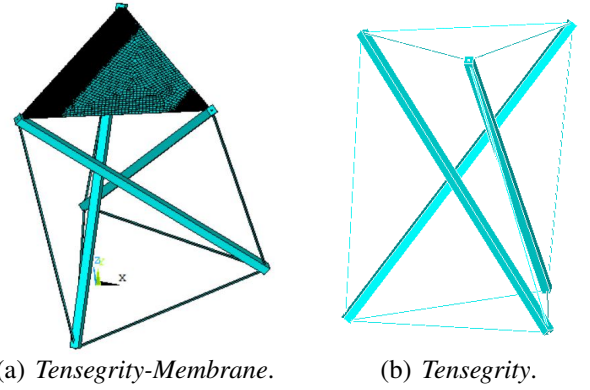


**Fig. 2** Tensegrity and Tensegrity-Membrane structures.

### 2.1 Dynamic Model of the system

A Finite Element model is used in order to obtain the dynamics characteristics of the structure. A bar element will be employed to represent the rods and cables of the tensegrity-membrane structure. The membrane will be modeled by shell elements.

#### 2.1.1 Bar element

The solution for the displacement of the bar element is given by:

$$u_{axial} = \omega_1 u_{axial_1} + \omega_2 u_{axial_2} \quad (29)$$

where the shape functions is described by  $\omega_1$  and  $\omega_2$ , and is given by:

$$\omega_1 = \frac{L - x}{L}, \quad (30)$$

and

$$\omega_2 = \frac{x}{L}, \quad (31)$$

where, the term  $x$  is the position on the element and  $L$  is its length.

The displacement interpolation matrix ( $\mathbf{H}$ ) organizes the shape functions. The matrix is presented in Equation 32:

$$\mathbf{H} = \begin{Bmatrix} \omega_1 \\ \omega_2 \end{Bmatrix} \quad (32)$$

The strain-displacement matrix  $\mathbf{B}$ , for the bar element, can be obtained by the Equation 33:

$$\mathbf{B} = \frac{\partial \mathbf{H}}{\partial x} \quad (33)$$

The stiffness matrix of an element is given by Equation 34, as shown in [15]:

$$\bar{\mathbf{k}}_e = \int_V \mathbf{B}^T \mathbf{C} \mathbf{B} dV \quad (34)$$

where  $\mathbf{C}$  is the material matrix and  $V$  is the element volume.

For the bar element,  $\mathbf{C} = E$  and  $V = AdL$ . Where  $E$  is the young's modulus and  $A$  is the area of the transversal cross section of the bar element.

As shown in [15], the mass matrix is given by:

$$\mathbf{M}_e = \int_V \rho \mathbf{H}^T \mathbf{H} dV \quad (35)$$

where  $\rho$  is the bar element density.

In local coordinates, the bar element is written as:

$$\mathbf{r}_e^T = [u_{axial1} \quad u_{axial2}] \quad (36)$$

The vector  $\mathbf{r}_e$  can be transformed into global coordinates  $\mathbf{R}_e$  by using the Equation 37:

$$\mathbf{R}_e = \mathbf{T}^T \mathbf{r}_e, \quad (37)$$

where  $\mathbf{T}$  is the transformation matrix with angles formed between the global and local coordinates. Then, the stiffness matrix can be written as:

$$\mathbf{K}_e = \mathbf{T}^T \bar{\mathbf{k}}_e \mathbf{T}, \quad (38)$$

The geometric stiffness matrix ( $\mathbf{K}_G$ ), presented in [14], is used in order to consider the pretensions applied in the cables and the bars of the tensegrity structure. The matrix ( $\mathbf{K}_G$ ) is presented in Equation 39.

$$\mathbf{K}_G = \mathbf{I} \otimes \mathbf{E} \quad (39)$$

where  $\mathbf{I}$  is the identity matrix and  $\mathbf{E}$  is the equilibrium matrix.

## 2.2 Shell element

In [15] is presented the shell element used in this paper. It's considered an isotropic material for the material matrix for the eight node element. Also, it's considered plane stress state.

## 3 Results and discussion

### 3.1 Finding the shape of the tensegrity structure

The desired configuration of the Tensegrity structure presents the shape observed in Figure 2(b).

The method of form-finding was implemented in the software Matlab<sup>TM</sup>. The initial force densities used in the adaptive force density method is shown in Table 1.

**Table 1** Initial force densities

	Force Density [N/m]
Base Tendons	1,2
Top Tendons	1,5
Vertical Tendons	2,5
Vertical Bar	2,5

It was imposed that each group of the structures (top, base and vertical members) had the same force densities between them. Also, it was imposed that the height of the structure has 150 mm.

The configuration obtained after 161 iterations is shown in Figure 3 and the position of the nodes in the Table 2.

The force densities and the final forces are shown in Table 3. Then, in order to the structure

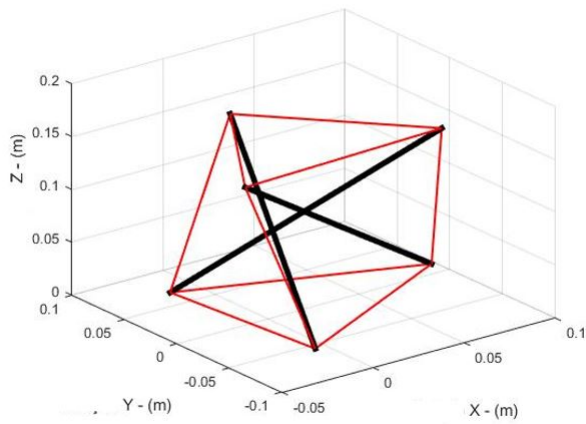


**Fig. 3** Configuration obtained with the force density method. The tendons are shown in red while the bars are represented in black.

**Table 2** Nodes obtained after 161 iterations.

Position [mm]	x	y	z
<b>Node 1</b>	97,8	13,7	0,0
<b>Node 2</b>	-14,0	68,9	0,0
<b>Node 3</b>	-5,9	-55,5	0,0
<b>Node 4</b>	-28,0	-27,0	15,0
<b>Node 5</b>	84,2	-19,7	15,0
<b>Node 6</b>	21,8	73,8	15,0

to have a desired configuration, the force densities of each member must maintain the same ratio as shown in Table 3.

**Table 3** Pretensions present in the final configuration of the structure.

	Force density [N/m]	Member lengths [mm]	Member forces [N]
<b>Base Tendons</b>	1,2558	125,7	0,1566
<b>Top Tendons</b>	1,5453	112,4	0,1737
<b>Vertical Tendons</b>	2,4129	154,3	0,3723
<b>Vertical Bars</b>	-2,4129	200,0	-0,4825

### 3.2 Modal analysis of the structure

The modal analysis was performed using a finite element model for the structure. Bar elements were used in the tendons and bars. Shell elements were used in the membrane. Also, in the simulation was considered the pretension of the structure.

The structure that was simulated consists of a membrane of  $51\mu\text{m}$ , a nylon cable of 1mm in diameter and a 5mm square steel bar. The material's properties used are presented in Table 4.

**Table 4** Properties of the materials used in the simulation

	Young's Modulus [GPa]	Poisson [-]	Density [kg/m <sup>3</sup> ]
<b>Nylon Tendons</b>	2	0,3	1130
<b>Steel Bars</b>	200	0,3	7800
<b>Membrane</b>	0,165	0,34	1400

#### 3.2.1 Pretension application

The addition of pretension in the longiline elements of the structure is simple. When consid-

ering stresses only in the axial direction, one has only to insert the stresses directly into the elements.

For the membrane, a static analysis is performed on the membrane. In this analysis, pressures are applied at the ends of the membrane and a restriction is applied at the center. The Figure 4(a) shows the constraints and forces applied. The force applied on the membrane is equivalent to the forces applied at the nodes of the structure, where the membrane will be fixed, so that the tensegrity has a stable configuration.

The average size of the 8-node shell elements is 2 mm. The average size of the elements for the refined mesh is approximately 0.6 mm.

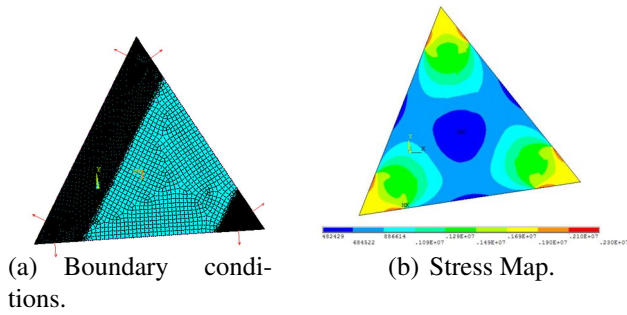


**Fig. 4** Boundary conditions for the membrane simulation and its stress map

When the stress map is obtained, as shown in Figure 4(b), it is inserted to the complete model shown in Figure 2(a).

### 3.2.2 Validation of the membrane simulation

In order to validate the membrane model, the numerical results of the prestressed membrane was compared with the experimental results obtained [1]. The simulation was carried out with a 22in.x23.25in.x0.002in. membrane with young's modulus of  $3.7 \times 10^5$  psi, mass density  $\rho = 2.7552$  slugs/ft<sup>3</sup>. The average size of the 8 node shell elements is 7mm. In order to account for the air influence in the experimental modal analysis, the mass density was multiplied by a factor of 2.6 [1]. It can be seen in Table 5 that the frequencies of the first mode has the greater difference between numerical and experimental

analysis. As shown in [16], in order to account for the air influence in the modal analysis, one could add mass to the model. The mass that is needed to be added is proportional to the wavelength of the membrane's vibrating mode. As the first vibrating mode has an greater wavelength, the air influence must be greater in this natural frequency, causing the difference in the results.

**Table 5** Comparison between numerical and experimental results.

Natural Frequency Numerical (Hz)	Natural Frequency Experimental [1] (Hz)
8.0	5.4
11.0	12.7
11.2	13.9
20.1	19.4

**Table 6** Comparison between numerical and experimental modes of vibration.

Mode of Vibration Numerical	Mode of vibration Experimental [1]

### 3.2.3 First vibration mode - with and without membrane

For this simulations, it was performed a modal analysis without fixation in the structure. The behavior of the first vibrating mode for the tensegrity and tensegrity-membrane structure is compared. The behavior of the natural frequency of the first mode of vibration in relation to the pretension applied in the vertical tendons can be seen in Figure 5.

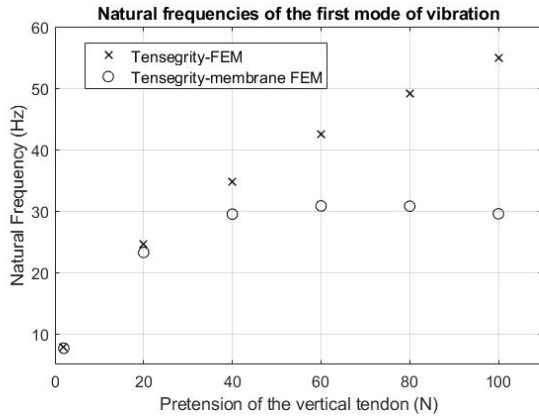


**Fig. 5** Behavior of the natural frequencies of the first modes of vibration in relation to the pretensions applied to the structure.

It can be seen from the Figure 5 that while the natural frequency of the first mode for the tensegrity structure, approximately, constantly grows as the pretension increases, the tensegrity-membrane presents a different behavior. One explanation would be the membrane inserted in the structure introduces new vibration modes whose natural frequencies become the lowest after a pretension of approximately 30 N. This can be verified in Figure 6 which plots the frequencies of two mode shapes, shown in Figure 7, for the tensegrity membrane structure and the first mode of vibration of the tensegrity structure. The mode shape will be the displacement configuration presented by the system during its vibration. It can be seen that the mode shape 2, inserted by the membrane, becomes the first mode of vibration at approximately 30 N. It can be seen that the mode shape 1 has similar behavior of the first mode of the tensegrity structure.

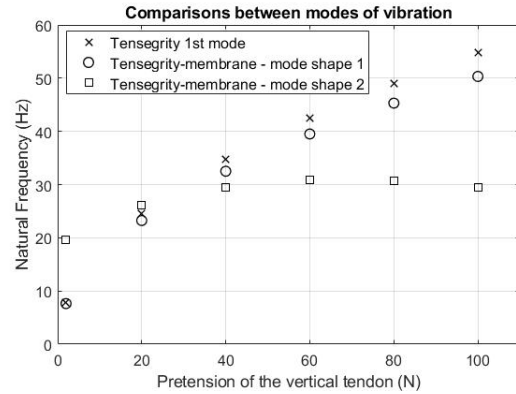


**Fig. 6** Behavior of natural frequencies of vibrating modes with corresponding shapes between tensegrity structures with and without membrane.

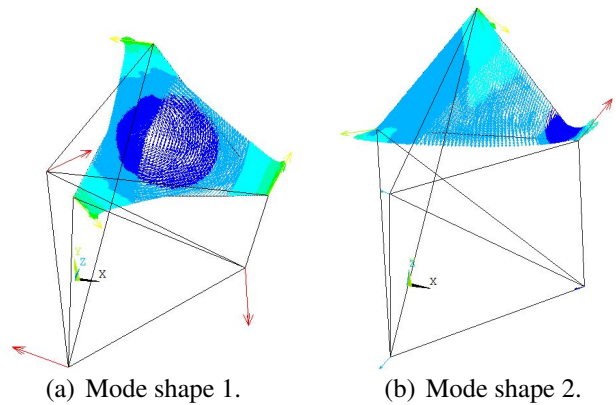


**Fig. 7** Mode shapes of the Tensegrity-membrane structure.

## 4 Conclusion

The force density method is quite efficient to find the forces of the tensegrity structures. With this method, it was possible to obtain the prestress and shape of the structure, indispensable for carrying out the modal analysis.

The addition of a membrane to exert the same function as the tendons may alter the behavior of the first vibration mode of the structure. It is noticed that the first mode, for the tensegrity-membrane has different behavior than that presented by the tensegrity structure. It's related to the mode shape introduced by the presence of the membrane.

## References

- [1] Young L G, Ramanathan S, Hu J and Pai P F. Numerical and experimental dynamic characteristics of thin-film membranes. *International Journal of Solids and Structures*, Vol. 42, No. 9, pp 3001-3025, 2005.
- [2] Fuller Richard Buckminster. *US Patent US3063521A*. 1962.
- [3] Paul C, Valero-Cuevas F J and Lipson H. Design and control of tensegrity robots for locomotion. *IEEE Transactions on Robotics*, Vol. 22, No. 5, pp 944-957, 2006.
- [4] Pugh, A. *an introduction to tensegrity*. University of California Press, 1976.
- [5] Kenneth D. Snelson. *US Patent US3169611A*. 1965.
- [6] Skelton, R E, de Oliveira, M. *Tensegrity Systems*. Springer US, 2009.
- [7] Yang, S and Sultan C. Modeling of tensegrity-membrane systems. *International Journal of Solids and Structures*, Vol. 82, pp 125-143, 2016.
- [8] Tibert, G. *Deployable Tensegrity Structures for Space Applications*. Phd Thesis, KTH, 2002.
- [9] Zhang J Y and Ohsaki, M. *Tensegrity Structures: Form, Stability and Symmetry*. 1st edition, Springer, 2015.
- [10] Connelly R. and Terrell M. Globally rigid Symmetric Tensegrities. *Structural Topology*, No. 21, pp 59-79, 1995.
- [11] Pellegrino, S. *Mechanics of kinematically indeterminate structures*. Phd Thesis, Cambridge University, 1986.
- [12] Schek H J. The force density method for form finding and computation of general networks. *Computer Methods in Applied Mechanics and Engineering*, Vol. 3, No. 1, pp 115-134, 1974.
- [13] Vassart N and Motro R. Multiparametered Formfinding Method: Application to Tensegrity Systems. *International Journal of Solids and Structures*, Vol. 14, No. 2, pp 125-143, 1999.
- [14] Zhang J Y and Ohsaki, M. Adaptive force density method for form-finding problem of tensegrity structures. *International Journal of Solids and Structures*, Vol. 43, No. 18, pp 5658-5673, 2006.
- [15] Bathe K. J. *Finite Element Procedures*. Prentice-Hall, 1996.
- [16] Kukathasan S and Pellegrino S. Vibration of Prestressed Membrane Structures in Air. *43RD AIAA/ASME/ASCE/AHS/ASC STRUCTURES, STRUCTURAL DYNAMICS, AND MATERIALS CONFERENCE*, Denver, pp 1-11, 2002.

## 5 Contact Author Email Address

Mail to: luishsteixeira@gmail.com

## Copyright Statement

The authors confirm that they, and/or their company or organization, hold copyright on all of the original material included in this paper. The authors also confirm that they have obtained permission, from the copyright holder of any third party material included in this paper, to publish it as part of their paper. The authors confirm that they give permission, or have obtained permission from the copyright holder of this paper, for the publication and distribution of this paper as part of the ICAS proceedings or as individual off-prints from the proceedings.